http://hdl.handle.net/1765/104869

Erasmus MC
Universitair Medisch Centrum Rotterdam

Hybrid Optical and CT Imaging reveals increased matrix metalloprotease activity and apoptosis preceding cardiac failure in progeroid *Ercc1* mice

Bibi S. van Thiel[1,2,3], Yanto Ridwan[1,3], Martine de Boer[4], Marion G.J. de Kleijnen[4], Nicole van Vliet[1], Paula M. van Heijningen[1], Wilbert P. Vermeij[1],
A.H. Jan Danser[3], Roland Kanaar[1,5], Dirk J. Duncker[4], Ingrid van der Pluijm[1,2], Jeroen Essers[1,2,5]

[1]Department of Molecular Genetics, Cancer Genomics Center Netherlands, [2]Department of Vascular Surgery, [3]Division of Vascular Medicine and Pharmacology, Department of Internal Medicine, [4]Division of Experimental Cardiology, Department of Cardiology, [5]Department of Radiation Oncology, Erasmus Medical Center, Rotterdam, The Netherlands

(Manuscript in preparation)

Erasmus University Rotterdam

ABSTRACT

In this study, we tested the use of functional micro-Computed Tomography (microCT) imaging combined with near infrared fluorescent (NIRF) probes to directly report the *in vivo* activity of key biomarkers of age-related cardiac failure using progeroid *Ercc1* mouse models. Mutations in the ERCC1 gene causes diminished DNA damage repair and an accelerated aging phenotype in mice, including cardiovascular aging. We tested the effect and kinetics of diminished DNA damage repair on protease activity and apoptosis and possible subsequent cardiac failure *in vivo*.

Full body *Ercc1*$^{d/-}$, cardiomyocyte-specific *Ercc1*$^{c/-}$ and their *Ercc1*-proficient controls were imaged with contrast enhanced microCT for anatomical reference and to assess cardiac morphology and function. The NIRF probes MMPSense680™ and Annexin-Vivo750™ were used to image matrix metalloprotease activity and apoptosis, respectively. Functional microCT analysis was compared to ultrasound imaging and results were validated by histology.

Ercc1$^{d/-}$ deficiency resulted in changes in left ventricular geometry and functioning at 24 weeks of age; an increase in left ventricular end-diastolic and left ventricular end-systolic volume was observed, thereby leading to an overall decrease in stroke volume and a substantial reduction in left ventricular ejection fraction. *Ercc1*-proficient mice showed relative stable volumes over time. Moreover, *Ercc1*$^{d/-}$ deficiency leads to increased myocardial apoptosis at 12 and 24 weeks of age, and a gradual increase of MMP activity already starting at 6 weeks, suggesting that these processes precede cardiac failure in these progeroid *Ercc1* mice. Cardiomyocyte-specific inactivation of *Ercc1* also led to impaired cardiac functioning and increased myocardial apoptosis and MMP activity, indicating that *Ercc1* deficiency in cardiomyocytes is associated with adverse cardiac remodeling and poor cardiac functioning.

In conclusion, combined microCT and optical imaging allows simultaneous analysis of molecular and functional changes in mouse models for accelerated aging and shows that gradual increases in matrix metalloprotease activity is followed by apoptosis and cardiac functional decline in progeroid *Ercc1* mice.

INTRODUCTION

Cardiovascular diseases (CVDs) persist as one of the leading causes of morbidity and mortality in the elderly population worldwide. The incidence and prevalence of numerous CVDs, including heart failure, myocardial infarction, atherosclerosis and hypertension, increase tremendously after the age of 50 years.[1, 2] Many hypotheses have been proposed to explain the aging process, but neither appears to be fully satisfactory.[3, 4] The accumulation of unrepaired DNA damage over time is regarded as one of the driving forces of accelerated aging and age-related diseases, as exemplified in mice and patients with genetic defects in DNA repair pathways.[5, 6] A variety of these genetically altered mice with affected DNA repair pathways, demonstrate a strict correlation between the severity of the DNA repair defect and the extend of aging pathology and reduced lifespan, suggesting that the load of DNA damage directly relates to the rate of aging.[6] Several lines of evidence, in experimental as well as clinical studies, support the notion that accumulation of DNA damage, secondary to oxidative stress, is involved in the development of age-related CVDs.[7] Yet, the precise role of DNA damage and related aging on the manifestation of CVDs remains elusive and needs further exploration.

One of the most widely studied mouse models of accelerated aging as a consequence of increased DNA damage is the *Ercc1*$^{d/-}$ mouse model. These mice contain one knockout allele of the Excision Repair Cross Complementation group 1 (*ERCC1*) gene, and one protein truncating mutation, in which the last seven amino acids at the C-terminus of the Ercc1 protein are deleted.[8] Due to this effect, these animals are deficient in multiple DNA repair mechanisms including global genome-and transcription-coupled nucleotide excision repair, interstrand crosslink repair and homologous recombination.[9] Consequently, DNA damage accumulation causes these mice to display an accelerated aging phenotype, including growth retardation, neurological degeneration and a shortened lifespan. In addition, *Ercc1*$^{d/-}$ mutants display accelerated age-dependent vasodilator dysfunction, increased vascular stiffness, increased blood pressure and vascular cell senescence.[10] Hence, these mice are useful to explore why DNA damage and aging are crucial components in CVD etiology.

Cardiac aging is a complex process in which many cellular and molecular changes occur in the heart, including increases in cardiomyocyte apoptosis, interstitial fibrosis and cardiomyocyte hypertrophy. At a functional level, aging is associated with an altered left ventricular (LV) diastolic function, diminished LV systolic reserve capacity, decreased blood flow and an increased prevalence of atrial fibrillation, eventually leading to a reduction in cardiac output and ejection fraction.[11] Loss of myocytes, through necrosis and apoptosis, has been demonstrated in the aging heart and is thought to contribute to the progressive loss of cardiac functioning.[12-14] Apoptosis is a tightly regulated cell death process that is an important contributor to the development of the cardiovascular

system as well as to the adaptation of the cardiovascular system to the continuous changing environment.[15, 16] Progressive apoptosis may lead to a dysbalance between cell death and cell renewal, eventually leading to cardiac decline and failure.[12, 13] It has been shown that unrepaired DNA damage is a trigger for a cell to undergo apoptosis, however, how this process contributes to a decline in cardiac performance remains to be elucidated. In addition to apoptosis, matrix metalloproteinases (MMPs) are found to participate in cardiac tissue remodeling in several CVDs, including myocardial infarction, heart failure and development of dilated cardiomyopathy (DCM).[17-20] MMPs are a family of proteolytic enzymes with the capacity to cleave components of the extracellular matrix, including elastin and collagen and thereby promote extracellular matrix turnover and degradation of the myocardial wall.[21] Clinical evidence suggests that MMP-9 has a significant role in LV remodeling and thus can serve as a novel prognostic biomarker for individuals at increased risk for CV mortality.[22-25] In this study, we therefore focused on apoptosis and MMP activity as potential biomarkers of age-related cardiac failure.

The most commonly used modality to evaluate cardiac functioning is echocardiography. However, functional analysis is performed in a 2D-view, and this generates a potential risk of inaccurate measurements of the whole heart, especially in small animals. In addition, assessment of right ventricular volumes and function remains challenging because of the particular shape of the right ventricle wrapped around the LV. This has been shown to be particularly unsatisfying in patients with non-standard ventricular size and anatomy.[26-28] Thus, there is a need for other noninvasive imaging techniques to evaluate CVDs. Contrast enhanced micro-Computed Tomography (microCT) imaging has been shown to be useful to investigate cardiac function and structure in small animals, as it has a high resolution and allows 3D imaging of heart and associated structures, providing reliable information about ventricular structure and function.[29] Moreover, the introduction of *in vivo* multimodality molecular imaging plays an increasingly pivotal role in biomedical and clinical research. MicroCT imaging can be combined with fluorescence molecular tomography (FMT) and near infrared fluorescent (NIRF) probe(s), which not only provides anatomical and functional data but also allows non-invasive studying of molecular targets involved in the development and progression of disease, including CVD, in small animals.[30-33] NIRF optical molecular imaging offers a new approach to evaluate processes involved in cardiac disease and provide valuable insights into different aspect of disease development and progression.

As *Ercc1* plays an important role in several DNA damage responses, we hypothesized that intact DNA repair in cardiomyocytes is critical for maintaining normal cardiac function and that complete or partial loss of *Ercc1* would provoke induced DNA damage, apoptosis and subsequent cardiac aging and failure. Furthermore, we tested the use of functional microCT imaging combined with NIRF probes targeting apoptosis and MMP

activity to directly report on the *in vivo* activity of these markers of age-related cardiac failure.

MATERIAL AND METHODS

Mouse model

All animal procedures were performed in accordance with the Principles of Laboratory Animal Care and Guidelines approved by the Dutch Animal Ethical Committee in full accordance with European legislation. As required by Dutch law, formal permission to generate and use genetically modified animals was obtained from the responsible local and national authorities. Animals were housed in individual ventilated cages under specific pathogen free conditions and maintained in a controlled environment (20-22°C, 12 h light: 12 h dark cycle). They were given *ad libitum* access to food (maintained on either AIN93G synthetic pellets (Research Diet Services B.V.; gross energy content 4.9 kcal/g dry mass, digestible energy 3.97 kcal/g) or standard chow diet) and water.

Male and female animals were used in this experiment. The generation of *Ercc1*$^{d/-}$ and *Ercc1*$^{+/+}$ mice has been described previously.[8] *Ercc1*$^{d/-}$ mutants (15% expression of the mutant Ercc1 allele), and their wild-type *Ercc1*$^{+/+}$ littermates (WT), in an F1 hybrid FVB/NJ x C57BL/6J background, were studied at 6, 12 and 24 weeks of age. Mice with a cardiomyocyte-specific deletion of *ERCC1* (αMHC-*Ercc1*$^{c/-}$) were generated using the *Cre-loxP* technology on a similar mixed background. Briefly, a floxed allele of *Ercc1* was generated by inserting loxP sites in intron 2 and 5, such that Cre recombinase excises exons 3–5 of the *Ercc1* locus.[34-36] Mice harboring two floxed alleles of *Ercc1* were crossed with hemizygous mice expressing Cre-recombinase under the control of the α-myosin heavy chain (αMHC-Cre) promotor. αMHC-*Ercc1*$^{c/-}$ and their control (cre^{-}) littermates were studied at 8 and 16 weeks of age.

In vivo microCT-FMT imaging of MMP activity and apoptosis

Mice were imaged with contrast enhanced Quantum FX Micro-computed Tomography (microCT) (Perkin Elmer Inc., Akron, Ohio, USA) for anatomical reference and to assess cardiac morphology and function. The NIRF probes MMPSense680™ and Annexin-Vivo750™ (Perkin Elmer Inc.) were used to image matrix metalloprotease (MMP) activity and apoptosis, respectively and imaged with the FMT 2500 fluorescence tomography *in vivo* imaging system (Perkin Elmer Inc.). The MMPsense probe is optically silent in a non-active state and becomes highly fluorescent following protease-mediated activation by MMPs, including MMP-2, -3, -9 and -13, whereas Annexin-Vivo binds to phosphatidylserine, which is exposed on the outer leaflet of the cell membrane lipid bilayer during the early stages of apoptosis. Briefly, mice were injected intravenously with MMPSense680™ (2 nmol/25 gram bodyweight in 100µl

PBS) 24 hours before microCT-FMT imaging. Mice were anaesthetized (1.5-2.5% isoflurane, O_2 1 L/min) and depilated to minimize the interference of fur on the fluorescent signal. 2 hours before FMT imaging, mice were injected intravenously with Annexin-Vivo750™. Before microCT imaging (Perkin Elmer Inc.), mice were injected in the tail vein with the iodinated contrast agent eXIA160 (Binitio Biomedical Inc., Ottawa, Canada), positioned in the imaging cassette and restrained to prevent movement during imaging. Mice were scanned using intrinsic cardiac respiratory gating to reduce artifacts caused by breathing or cardiac motion. After microCT imaging, mice remained under anesthesia and the cassette was transferred to the FMT 2500 fluorescent tomography *in vivo* imaging system (Perkin Elmer Inc.). FMT imaging was performed using 680 and 700 nm excitation and emission wavelengths, respectively, 24 hours after injection of MMPSense680™. The multimodal animal cassette facilitates the coregistration of FMT and CT data through fiducial landmarks. FMT and microCT data were merged using the Amide software and *in vivo* fluorescence was quantified. Functional parameters were calculated from the 3D microCT images with the help of the software ANALYZE® 12.0 (AnalyzeDirect Inc., Overland Parks, KS, USA).

Ex vivo fluorescent imaging of excised hearts

After *in vivo* microCT-FMT imaging, mice were euthanized using an overdose of inhalant anesthetic isoflurane. Hearts were excised, emersion fixed in formalin and assessed for *ex vivo* tissue epifluorescence using the FMT system and the Odyssey® CLx imaging system (LI-COR® Biosciences, Lincoln, Nebraska, USA).

Statistical analysis

Data are expressed as the mean±SEM. Differences between groups were evaluated by Student's t-test or ANOVA, and corrected for multiple testing by post-hoc Bonferroni analysis when needed. P<0.05 was considered significant. All analyses were performed using IBM SPSS Statistics version 20.0 (SPSS Inc., Chicago, IL, USA).

RESULTS

Ercc1 deficiency results in changes in LV geometry and functioning

As previously described, *Ercc1*$^{d/-}$ mice showed reduced growth, declined body weight and a shortened lifespan (of approximately half a year) compared to their control littermates (Fig. 1a and 1b, and Table 1).[37] To investigate the effect of *Ercc1*$^{d/-}$ deficiency on heart geometry and function, anesthetized mice were injected with an iodinated contrast agent and imaged with the use of microCT. Imaging revealed an enlargement of the heart chambers in *Ercc1*$^{d/-}$ animals at 24 weeks of age compared to *Ercc1*$^{d/-}$ animals at 6 and 12 weeks of age. This was in striking contrast to the relatively stable volumes in the WT group over time, shown by a

volumetric 2D representation of the heart in end-diastole (Fig. 1c). To investigate whether normal cardiac function is maintained in *Ercc1*$^{d/-}$ mice, LV parameters were analyzed. *Ercc1*$^{d/-}$ mice showed an increase in left ventricular end-diastolic (LVED) volume (24-week-old *Ercc1*$^{d/-}$ 33+/-1 mm^3 versus 6-week-old *Ercc1*$^{d/-}$ 27+/-2 mm^3; p<0.05; n=22 and n=6, respectively), suggesting that the LV chamber is 24% dilated in diastole at 24 weeks of age compared to the earlier time points (Fig. 1d and Table 1). In addition, an increase in left ventricular end-

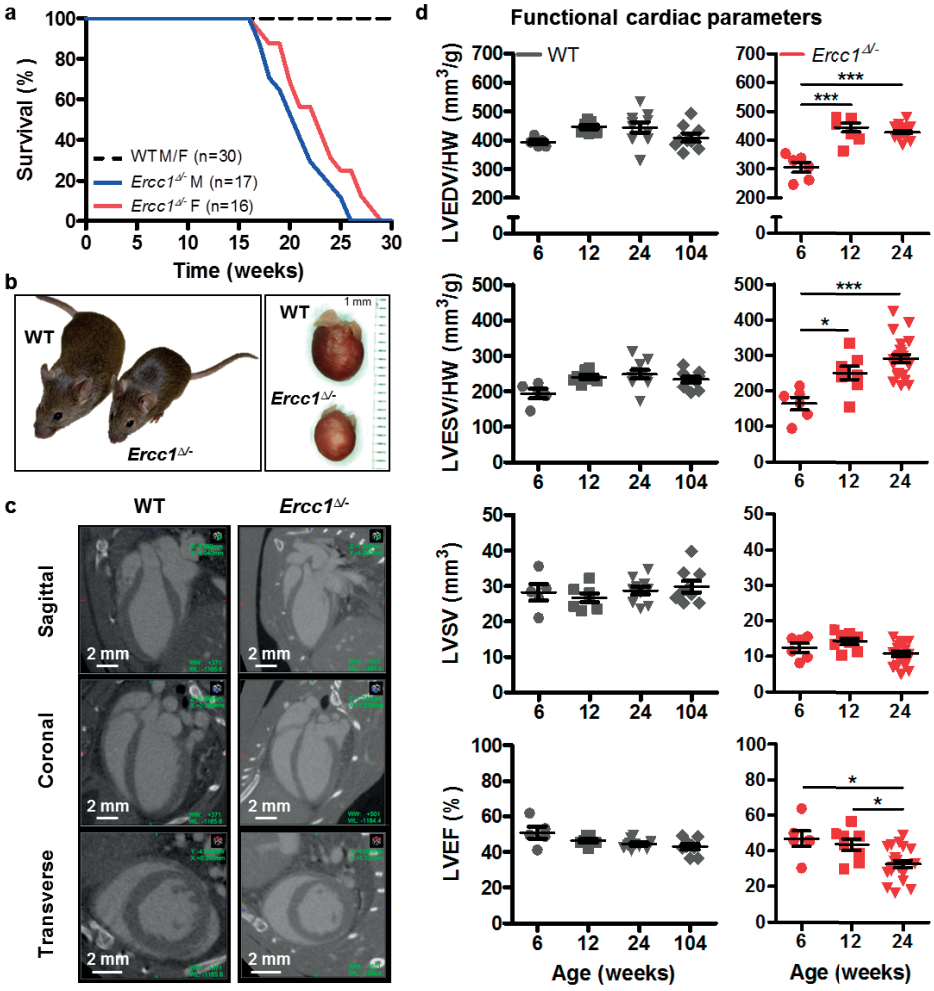

Figure 1. *Ercc1* deficiency results in a shortened lifespan and a deterioration in left ventricular function (LV) at 24 weeks of age. a. Lifespan is reduced in *Ercc1*$^{d/-}$ mice compared to control littermates. b. Representative pictures of WT and *Ercc1*$^{d/-}$ mice and hearts at the age of 24 weeks. c. Representative microCT images of the heart in left ventricular end-diastole from WT and *Ercc1*$^{d/-}$ mice at 24 weeks of age. d. MicroCT functional imaging revealed a deterioration in LV function in *Ercc1*$^{d/-}$ at 24 weeks of age. Data is presented as mean±SEM. Statistical significance *P<0.05 and **P< 0.001.

systolic (LVES) volume was observed, leading to an overall decrease in stroke volume at 24 weeks (24-week-old *Ercc1*$^{d/-}$ 22+/-1 mm^3 versus 6-week-old *Ercc1*$^{d/-}$ 14+/-2 mm^3; p<0.05; n=22 and n=6, respectively). WT mice showed stable volumes over time. Because stroke volume decreased while LVED volume increased in *Ercc1*$^{d/-}$ mice at the age of 24 weeks, there is a substantial reduction in left ventricular ejection fraction (LVEF) (24-week-old *Ercc1*$^{d/-}$ 33%+/-2 versus WT 44%+/-1; p<0.05; n=22 and n=10, respectively).

Table 1. Left ventricular volumes and global functional indices measured in 6- and 24-week-old WT and *Ercc1*$^{d/-}$ mice. Data represents mean±SEM. Statistical significance *P<0.05 and **P< 0.01. LVEDV, left ventricular end-diastolic volume; LVESV, left ventricular end-systolic volume; LVSV, left ventricular stroke volume; LVEF, left ventricular ejection fraction; LVMV, total left ventricular myocardial volume; LVMM, left ventricular myocardial mass; BPM, beats per minute.

	Control WT			Mutant *Ercc1*$^{\Delta/-}$		
	6 weeks	**24 weeks**	**Δ %**	**6 weeks**	**24 weeks**	**Δ %**
Body weight (g)	26.1 ± 1.38 M 20.7 ± 0.20 F	43.4 ± 1.01 M 28.6 ± 1.42 F	+16 -2	17.3 ± 0.89 M 13.7 ± 0.50 F	13.5 ± 0.32 M 13.3 ± 0.23 F	-13 -10
Heart weight (g)	0.139 ± 0.005	0.148 ± 0.008	+6	0.087 ± 0.003	0.077 ± 0.001	-12
LVEDV (mm^3)	54.69 ± 1.53	64.71 ± 2.27	+18	26.68 ± 1.69	33.00 ± 0.55	+24**
LVESV (mm^3)	26.74 ± 1.50	36.02 ± 1.39	+35	14.25 ± 1.52	22.16 ± 0.80	+55**
LVSV (mm^3)	27.94 ± 2.39	28.69 ± 1.12	+3	12.43 ± 1.26	10.84 ± 0.69	-13
LVEF (%)	50.87 ± 3.35	44.35 ± 0.85	-13	46.82 ± 4.36	32.87 ± 2.10	-30*
LVMV (mm^3)	81.92 ± 3.63	93.62 ± 9.30	+14	49.98 ± 2.59	46.25 ± 1.46	-7
LVMM (mg)	86.02 ± 3.81	93.30 ± 9.76	+14	52.48 ± 2.72	48.56 ± 1.53	-7

Cardiomyocyte-specific deletion of *Ercc1* in the heart leads to impaired cardiac functioning

In order to investigate whether the observed cardiac impairment in the *Ercc1*$^{d/-}$ animals was due to loss of *Ercc1* in the heart or due to overall age-related systemic organ failure, *Ercc1* was deleted specifically in the cardiomyocytes of the heart. These αMHC-*Ercc1*$^{c/-}$ mice exhibited normal growth and body weight, similar to control (Table 2), but subsequently showed a reduced lifespan of about 24 weeks (Fig. 2a). From 16 weeks on an overall decrease in health and survival was observed. Therefore, cardiac size and function were assessed with microCT in 8 and 16-week-old αMHC-*Ercc1*$^{c/-}$ and control mice. At 16 weeks, αMHC-*Ercc1*$^{c/-}$ showed an increase in LVED volume (*Ercc1*$^{c/-}$ 73+/-6 mm^3 versus WT 57+/-3 mm^3; p<0.05; n=4 both groups) as well as an increase in LVES volume (*Ercc1*$^{c/-}$ 51+/-5 mm^3 versus WT 29+/-3 mm^3; p<0.05; n=4 both groups). This suggest that left ventricular dilation and systolic dysfunction were present in αMHC-*Ercc1*$^{c/-}$ at 16 weeks of age (Fig. 2c). The deterioration of LV function in αMHC-*Ercc1*$^{c/-}$ mice preceded signs of heart failure (*Ercc1*$^{c/-}$ 30%+/-1 versus WT 50%+/-2; p<0.05; n=6 both groups) (Fig. 2c). These results indicate that *Ercc1* deficiency in cardiomyocytes is associated with adverse cardiac remodeling and poor cardiac functioning.

Table 2. Left ventricular volumes and global functional indices measured in 8- and 16-week-old control and αMHC-*Ercc1*$^{c/-}$ mice. Data represents mean ± SEM. Statistical significance *P<0.05 and **P< 0.01. LVEDV, left ventricular end-diastolic volume; LVESV, left ventricular end-systolic volume; LVSV, left ventricular stroke volume; LVEF, left ventricular ejection fraction; BPM, beats per minute.

	Control Cre-			aMHC-*Ercc1*$^{c/-}$		
	8 weeks	**16 weeks**	**Δ %**	**8 weeks**	**16 weeks**	**Δ %**
Body weight (g)	22.7 ± 1.2	27.8 ± 3.3	+22	21.3 ± 2.1	24.2 ± 2.2	+14
Heart weight (g)	0.111 ± 0.004	0.136 ± 0.007	+22	0.112 ± 0.008	0.130 ± 0.008	+16
LVEDV (mm^3)	46.91 ± 1.59	57.26 ± 2.98	+22	50.55 ± 3.07	72.48 ± 5.76	+43
LVESV (mm^3)	25.08 ± 1.12	28.85 ± 2.63	+15	29.49 ± 2.25	50.85 ± 4.43	+72
LVSV (mm^3)	21.83 ± 1.47	28.42 ± 1.01	+30	21.06 ± 0.82	21.63 ± 1.18	+3
LVEF (%)	46.46 ± 2.14	50.10 ± 2.29	+8	41.76 ± 0.88	29.97 ± 1.18	-28

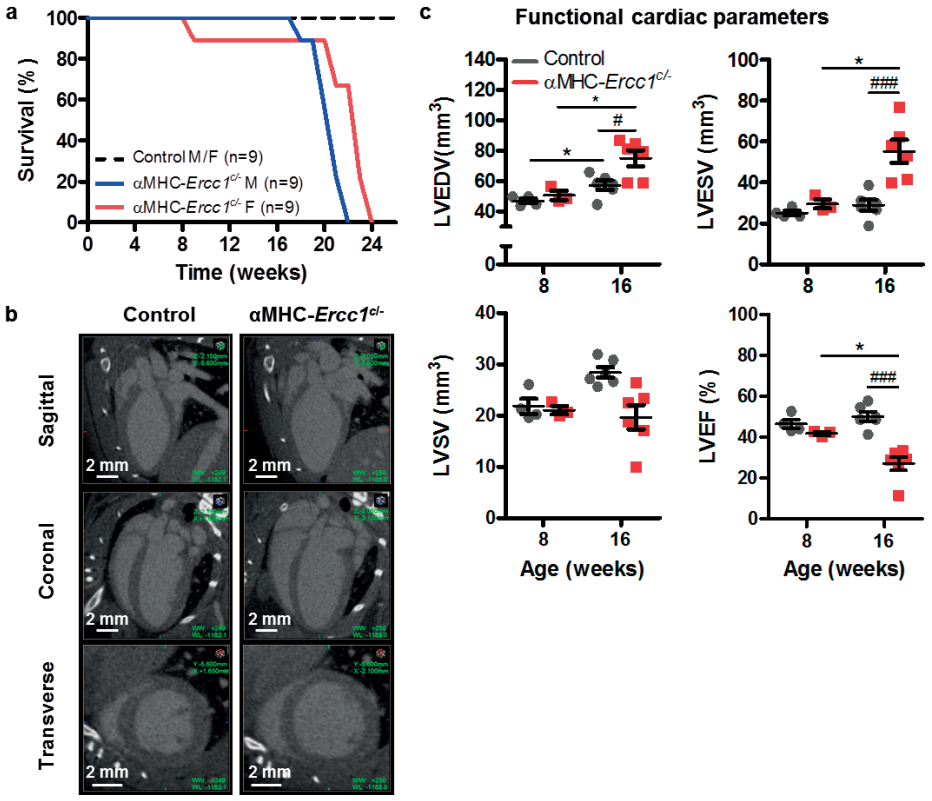

Figure 2. Specific deletion of Ercc1 in cardiomyocytes leads to early onset of left ventricular (LV) dysfunction. a. Specific loss of *Ercc1* in cardiomyocytes (αMHC-*Ercc1*$^{c/-}$) leads to a significant reduction in lifespan compared to littermate controls. b. Representative microCT images of the heart from αMHC-*Ercc1*$^{c/-}$ mouse and control littermates, showing an increase in size of the heart from the mutant animals at the age of 16 weeks. c. MicroCT functional imaging revealed that left ventricular function is impaired in αMHC-*Ercc1*$^{c/-}$ mice. Data is presented as mean±SEM. Statistical significance *P<0.05 and **P< 0.001.

Ercc1 deficiency causes a gradual decrease in LV myocardial mass over time

As a lot of patients diagnosed with heart failure have an underlying type of cardiomyopathy, i.e. disease of the myocardium, we quantified the myocardial wall volume and mass in *Ercc1*$^{d/-}$ hearts of 6, 12 and 24 weeks of age, using the microCT data (as indicated in Fig. 3a). 3D-reconstructed myocardial wall images showed a gradual decrease in myocardial mass in *Ercc1*$^{d/-}$ hearts over time (Fig. 3b). Quantification of the LV wall mass confirmed LV myocardial wall thinning in *Ercc1*$^{d/-}$ hearts at 24 weeks of age compared to 6-week-old *Ercc1*$^{d/-}$ mice, whereas the LV myocardial wall mass of WT mice increased from 6 until 24 weeks of age (Fig. 3c).

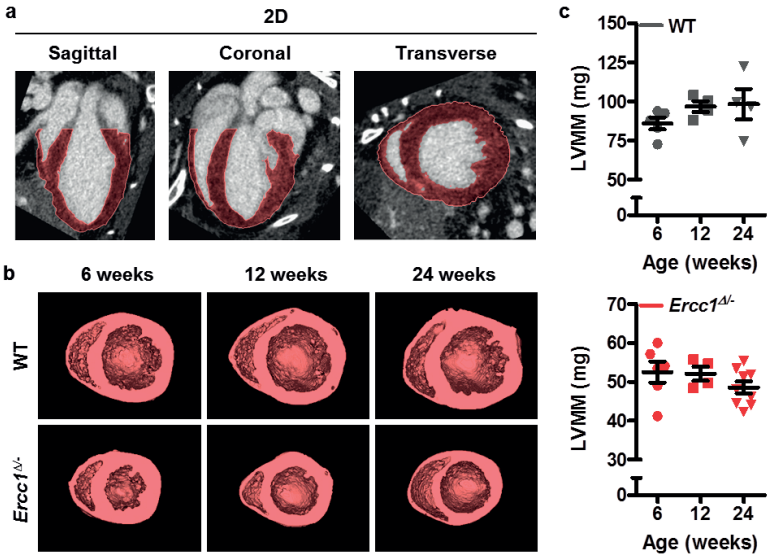

Figure 3. *Ercc1*$^{D/-}$ mice causes a gradual decrease in LV myocardial mass over time. a. Representative microCT images of a WT heart in which the myocardial wall is selected (red) for analysis. b. 3D reconstructed myocardial wall images of WT and *Ercc1*$^{d/-}$hearts over time show a gradual thinning of the myocardial wall in 24-week-old *Ercc1*$^{d/-}$hearts. c. Quantification of the left ventricular (LV) wall mass confirmed a trend in LV myocardial wall thinning in *Ercc1*$^{d/-}$ hearts at 24 weeks of age. Data is presented as mean±SEM. Statistical significance *P<0.05 and **P< 0.001.

Ercc1 deficiency leads to increased myocardial apoptosis and MMP activity

To investigate whether we could, non-invasively, detect apoptotic cells in the aging *Ercc1*$^{d/-}$ hearts, we injected these animals with the NIRF probe Annexin-Vivo750™ that binds to phosphatidylserine which is exposed on the outer leaflet of the cell membrane lipid bilayer during the early stages of apoptosis. MicroCT-FMT-reconstructed 3D images showed an increased intensity of Annexin-Vivo in *Ercc1*$^{d/-}$ compared to WT mice, at 24 weeks of age (Fig. 4a). Quantification of the *in vivo* fluorescent signal revealed significantly increased myocardial apoptosis in *Ercc1*$^{d/-}$ mice at all ages when compared to WT (24 weeks 164+/-25

versus 16+/-3 pmol/g, respectively; p<0.001; n=8 vs n=5) (Fig. 4b). 2D tissue epifluorescence imaging of excised hearts confirmed the increased fluorescence seen noninvasively by FMT in the *Ercc1*$^{d/-}$ mice (Fig. 4c and d). In addition, representative heart sections were

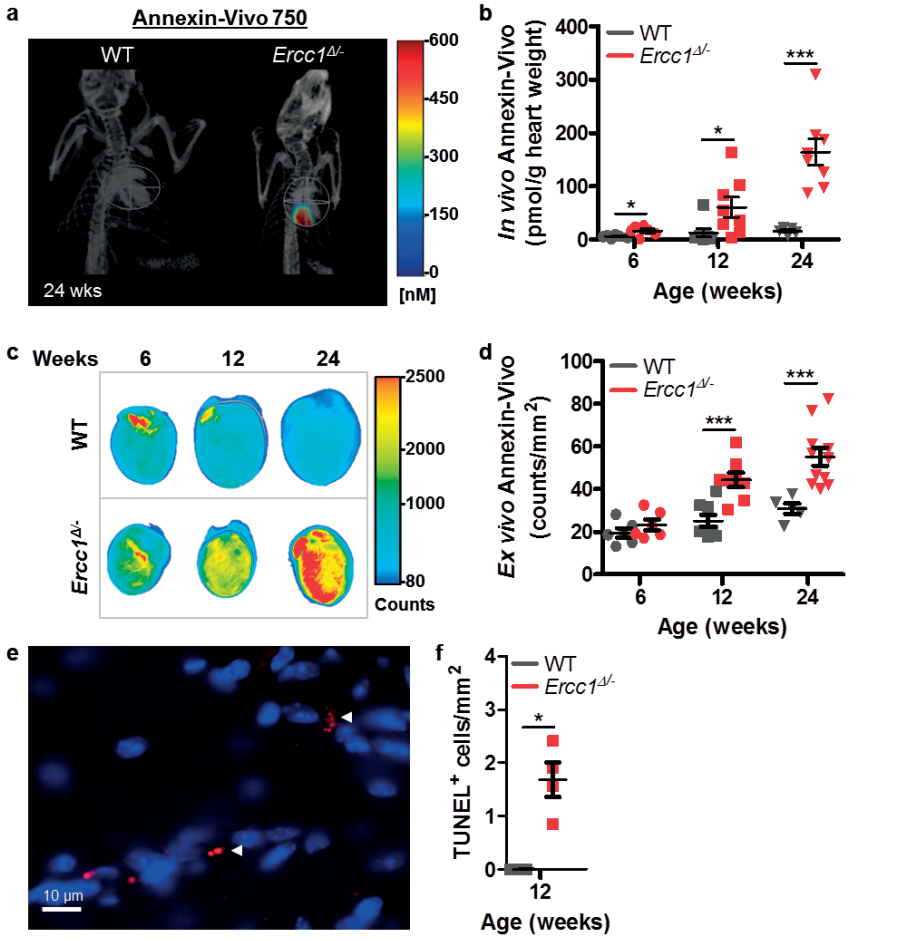

Figure 4. *Ercc1* deficiency leads to increased myocardial apoptosis. a. *In vivo* fluorescent imaging of apoptosis in the heart in *Ercc1*$^{d/-}$ mice compared to WT, at 24 weeks of age. Signal from the other tissues is excluded for clarity. b. *In vivo* quantitative data, by dual fusion of FMT and CT imaging, revealed increased myocardial apoptosis in *Ercc1*$^{d/-}$ mice at 12 and 24 weeks of age. c. Epifluorescence images of the heart, obtained with an odyssey imaging system, show an increase in apoptotic signal at 24 weeks of age in the *Ercc1*$^{d/-}$ mice compared to WT. d. Quantification of 2D tissue epifluorescence imaging of excised hearts confirmed the increased fluorescence in the *Ercc1*$^{d/-}$ mice. e. Representative heart sections showed that the NIRF fluorescence of the injected Annexin-Vivo probe was detected on the membrane of cells. f. Immunohistochemistry confirmed the presence of apoptotic cells in the myocardium of 12 and 18 weeks old *Ercc1*$^{d/-}$ mice. Data is presented as mean±SEM. Statistical significance *P<0.05 and **P< 0.001

examined under a fluorescent microscope, which showed that the NIRF fluorescence of the injected Annexin-Vivo probe was detected on the membrane of cells (Fig. 4e). Immunohistochemistry confirmed the presence of apoptotic cells in the myocardium of 12 weeks old *Ercc1*$^{d/-}$ mice (Fig. 4f). TUNEL staining revealed a greater occurrence of apoptotic myocytes in *Ercc1*$^{d/-}$ hearts, whereas only a few TUNEL-positive cells were detected in WT hearts. Apoptotic cells were located throughout the whole myocardium. As shown in Figure 4f, quantification of cardiomyocyte apoptosis by TUNEL staining demonstrated an approximate 2-fold increase in *Ercc1*$^{d/-}$ hearts compared to WT hearts. Since MMPs participate in cardiac remodeling after acute injury and are involved in the breakdown of the myocardium, we injected the accelerated aging *Ercc1*$^{d/-}$ mice with the MMP-specific activatable NIRF probe MMPSense680™ to detect possibly increased MMP activity in the *Ercc1*$^{d/-}$ hearts. We subsequently determined tissue epifluorescence levels in excised hearts using the Odyssey imaging system. At 6 and 24 weeks of age, *Ercc1*$^{d-}$ hearts showed increased MMP activity compared to WT hearts (Fig. 5a and b).

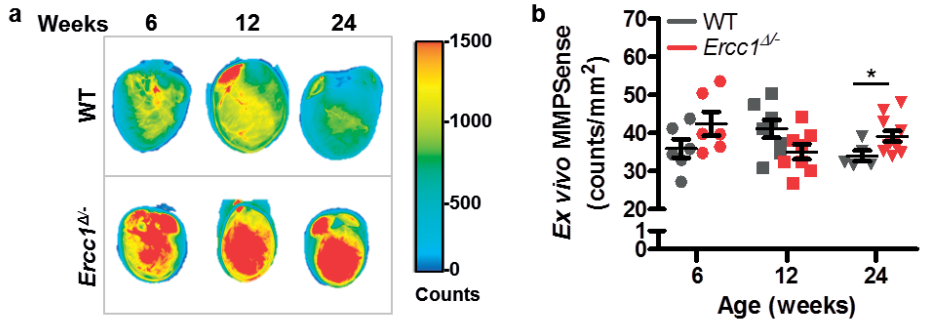

Figure 5. *Ercc1* deficiency results in a gradual increase of MMP activity in the myocardium. a. 2D Tissue epifluorescence imaging of excised hearts using the Odyssey imaging system. b. Quantification of epifluorescence imaging of excised hearts showed a significant gradual increase of MMP activity at 24 weeks of age, in the *Ercc1*$^{d/-}$ mice compared to WT. Data is presented as mean±SEM. Statistical significance *P<0.05 and **P< 0.001.

DISCUSSION

Research focusing on age-related diseases in humans carries unique challenges, because of its complexity as well as the time involved, thus the need remains for preclinical studies based on animal models that resemble the clinical setting of age-related diseases at accelerated pace. During the past few decades, many animal models to study certain aspects of cardiac aging and related disease have emerged, however, the precise role of DNA repair deficiency and related accelerated aging on CVD remains largely elusive.[38, 39] As accumulation of DNA damage is regarded as one of the possible explanations of aging, in this study

we explored the effect of *Ercc1* deficiency, leading to defects in DNA repair, on cardiac function.[4] We evaluated cardiac performance starting at 6 through 24 weeks of age using non-invasive microCT imaging. Additionally, we tested the use of functional microCT imaging combined with NIRF probes to explore whether we could directly report on the *in vivo* activity of MMP and the occurrence of apoptosis in the aging heart, and investigated if these probes can serve as markers for age-related CVD.

In the present study, we demonstrate that *Ercc1* deficiency results in changes in geometry and functioning of the heart with age. Adult *Ercc1*$^{d/-}$ mice exhibited ventricular chamber enlargement and LV myocardial wall thinning, however decreased stroke volume/ejection fraction only occurred at the end of their lifespan (24 weeks). The overall changes in the heart and myocardium of the 24-week-old *Ercc1*$^{d/-}$ mice suggest that *Ercc1* deficiency contributes to the development of features consistent with progressive DCM, a common pathology seen in aged humans.[40] DCM is a disease of the myocardium that is characterized by ventricular chamber enlargement with a reduction in cardiac performance, often accompanied by progressive thinning of the myocardial wall. Several studies have already indicated a link between DNA damage and DCM in humans as well animal models. Patients with DCM, exhibited elevated levels of 8-hydroxy-2-deoxyguanosine (8-OhdG) in their serum and myocardium, suggesting an increase in overall oxidative DNA damage in this type of cardiac disease.[41] Moreover, mitochondrial DNA damage and dysfunction have been shown to activate apoptosis and cause DCM.[42-44] DNA damage and aging are not limited to DCM, but also contribute to other types of CVDs, including heart failure and myocardial infarction.[45-49] In addition, increasing evidence indicates that therapeutic radiation treatment causes various types of DNA damage and consequently can cause cardiovascular complications (reviewed within Ishida et al.).[46]

The *Ercc1*$^{d/-}$ mouse model has been well recognized as a model of accelerated aging, and as such the pathology observed in these animals could be the result of accelerated systemic organ aging and consequent failure.[6, 37] However, as we showed that cardiomyocyte-specific deletion of *Ercc1* identically impaired cardiac functioning, we conclude that *Ercc1* deficiency in the heart results in adverse cardiac remodeling and poor cardiac functioning, independently of overall age-related systemic organ failure. Mice with cardiomyocyte-specific deletion of *Ercc1* had an overall lifespan approximately 20 weeks and likely died due to the decrease in cardiac performance. However, only at 24 weeks of age the Ercc1$^{d/-}$ mice showed a decrease in LVEF. We chose 24 weeks as our end-point because it has been previously reported that *Ercc1*$^{d/-}$mice have an average lifespan of 24-28 weeks, as shown in Figure 1a.[37, 50, 51] During their lifetime, these *Ercc1*$^{d/-}$ animals show numerous accelerated aging features including loss of vision and hearing, dystonia and tremors, kyphosis, ataxia and progressive neurodegeneration.[50, 52, 53] The exact cause of death in these mice is still unknown, but is probably related to the fact that the most vulnerable organ systems fail first, thus preventing information acquisition of the aging phenotype on other organ

systems, including the heart. Nevertheless, the vast amount on functional, histopathological, transcriptional, proteomic, metabolomics and ultrastructural data regarding the *Ercc1*$^{d/-}$ mice support the conclusion that these animals copy normal murine aging, and are a useful model to study the effect of aging and DNA repair defects on disease development and progression (reviewed within Gurkar et al.).[54]

Hybrid imaging optimized for small animals is very important because of the widespread use of genetically engineered mice resembling disease and the need to *in vivo* investigate the functional, anatomical and molecular phenotype of these mice. Imaging of the cardiovascular system, especially the right ventricle and the myocardial wall, has been quite challenging for a long time. The advances in new and existing imaging modalities for small animals, allow more accurate, high resolution, 3D, longitudinal imaging of the cardiovascular system and provides rapid translation of new knowledge to the clinic.[55] MicroCT imaging is frequently used for characterization of cardiac function and structure in small animals, and current systems now provide cardio-respiratory gating, to minimize movement interference.[56, 57] The current study used microCT imaging not only to determine cardiac function but also explore the shape and anatomy of the myocardial wall. We could accurately measure the myocardial wall volume and mass, demonstrating that *Ercc1*$^{d/-}$ mice show myocardial wall thinning at 24 weeks of age. Moreover, representative microCT images of the *Ercc1*$^{d/-}$ hearts suggest that the right ventricle is also affected in these mice, and analysis and quantification thereof should give us more answers regarding the function and geometry of the right ventricle. The microCT is well suited for examination of cardiac disease in small animals.

Fluorescent molecular imaging data presented in this study revealed that cardiac aging and subsequent failure in the progeroid *Ercc1* mice is preceded by a gradual increase in MMP activity and an increase in apoptosis. Aging is linked to increased MMP activity and extracellular matrix turnover, which could lead to myocardial remodeling thereby affecting cardiac performance. Several different types of MMPs are detected in diseased hearts, in which MMP-9, in particular, is found to play a key role.[24, 58, 59] However, the suggestion that MMP-9 can serve as potential plasma markers for cardiac aging might not be correct, as the age-associated increase of circulating MMP-9 in mice is in contrast with the decrease of circulating MMP-9 found in aging humans.[60, 61] This highlights the complexity of the presence and role of MMPs in age-related diseases. The MMPs found in the aging heart might be derived from senescent cells and due to the senescence-associated secretory phenotype.[62] Numerous examples of increased cellular senescence involved in age-related pathology have been reported.[63] DNA damage is a crucial mediator for cells to undergo apoptosis or enter senescence and it was shown that *Ercc1* deficient cells undergo premature cellular senescence.[8] Hence, the increased MMP activity observed in *Ercc1*$^{d/-}$ mice might also be derived from senescent cells, and the use of *in vivo* molecular imaging of MMP activity could help to follow changes in activity over time. Additionally, apoptosis

has been suggested to be responsible for a significant amount of cardiomyocyte death that contributes to the development and progression of heart failure. Indeed, apoptosis has been found in several cardiac diseases.[64-66] However, whether there are increases in apoptotic cells in failing hearts remains controversial.[67] One of the arguments is that the TUNEL technique, which detect apoptosis by identifying *in situ* DNA nicks, is not solely specific for programmed cell death but might also label cells that undergo DNA repair.[68] The apoptosis probe we used in this study, Annexin-Vivo750™, binds to phosphatidylserines exposed on the outside of early apoptotic cells and does not detect DNA nicks, and therefore holds potential for *in vivo* identification of apoptosis. Fluorescent imaging of Annexin-Vivo in the *Ercc1*$^{d/-}$ mice, demonstrated that *Ercc1* deficiency leads to increased myocardial apoptosis already starting at 6 weeks of age before changes in cardiac performance occurred. Accordingly, this probe holds important potential for *in vivo* assessment of apoptosis involved in CVDs and can provide valuable insights into early disease detection. Prevention of cardiovascular disease requires early detection and risk stratification before the manifestation of disease.

In conclusion, this is the first study to show that *Ercc1* deficient accelerated aging mice develop cardiac pathology which starts with an *in vivo* gradual increase in MMP activity followed by apoptosis, leading to progressive ventricular enlargement, LV myocardial wall thinning and reduction in cardiac performance. The use of microCT is a valuable imaging modality to establish cardiac function in small animals as well as explore 3D geometric changes throughout the heart. Moreover, combined CT and optical imaging allows simultaneous analysis of molecular and functional changes in mouse models for accelerated aging and hold important potential for early disease detection, exploring disease progression and the assessment of therapeutic effects.

REFERENCES

1. Benjamin EJ, Blaha MJ, Chiuve SE, Cushman M, Das SR, Deo R, de Ferranti SD, Floyd J, Fornage M, Gillespie C, Isasi CR, Jimenez MC, Jordan LC, Judd SE, Lackland D, Lichtman JH, Lisabeth L, Liu S, Longenecker CT, Mackey RH, Matsushita K, Mozaffarian D, Mussolino ME, Nasir K, Neumar RW, Palaniappan L, Pandey DK, Thiagarajan RR, Reeves MJ, Ritchey M, Rodriguez CJ, Roth GA, Rosamond WD, Sasson C, Towfighi A, Tsao CW, Turner MB, Virani SS, Voeks JH, Willey JZ, Wilkins JT, Wu JH, Alger HM, Wong SS, Muntner P, American Heart Association Statistics C, Stroke Statistics S. Heart disease and stroke statistics-2017 update: A report from the american heart association. *Circulation*. 2017;135:e146-e603
2. Niccoli T, Partridge L. Ageing as a risk factor for disease. *Curr Biol*. 2012;22:R741-752
3. Jin K. Modern biological theories of aging. *Aging Dis*. 2010;1:72-74
4. Lopez-Otin C, Blasco MA, Partridge L, Serrano M, Kroemer G. The hallmarks of aging. *Cell*. 2013;153:1194-1217

5. Garinis GA, van der Horst GT, Vijg J, Hoeijmakers JH. DNA damage and ageing: New-age ideas for an age-old problem. *Nat Cell Biol*. 2008;10:1241-1247
6. Vermeij WP, Hoeijmakers JH, Pothof J. Genome integrity in aging: Human syndromes, mouse models, and therapeutic options. *Annu Rev Pharmacol Toxicol*. 2016;56:427-445
7. De Flora S, Izzotti A. Mutagenesis and cardiovascular diseases molecular mechanisms, risk factors, and protective factors. *Mutat Res*. 2007;621:5-17
8. Weeda G, Donker I, de Wit J, Morreau H, Janssens R, Vissers CJ, Nigg A, van Steeg H, Bootsma D, Hoeijmakers JH. Disruption of mouse ercc1 results in a novel repair syndrome with growth failure, nuclear abnormalities and senescence. *Curr Biol*. 1997;7:427-439
9. Niedernhofer LJ, Garinis GA, Raams A, Lalai AS, Robinson AR, Appeldoorn E, Odijk H, Oostendorp R, Ahmad A, van Leeuwen W, Theil AF, Vermeulen W, van der Horst GT, Meinecke P, Kleijer WJ, Vijg J, Jaspers NG, Hoeijmakers JH. A new progeroid syndrome reveals that genotoxic stress suppresses the somatotroph axis. *Nature*. 2006;444:1038-1043
10. Durik M, Kavousi M, van der Pluijm I, Isaacs A, Cheng C, Verdonk K, Loot AE, Oeseburg H, Bhaggoe UM, Leijten F, van Veghel R, de Vries R, Rudez G, Brandt R, Ridwan YR, van Deel ED, de Boer M, Tempel D, Fleming I, Mitchell GF, Verwoert GC, Tarasov KV, Uitterlinden AG, Hofman A, Duckers HJ, van Duijn CM, Oostra BA, Witteman JC, Duncker DJ, Danser AH, Hoeijmakers JH, Roks AJ. Nucleotide excision DNA repair is associated with age-related vascular dysfunction. *Circulation*. 2012;126:468-478
11. North BJ, Sinclair DA. The intersection between aging and cardiovascular disease. *Circ Res*. 2012;110:1097-1108
12. Foo RS, Mani K, Kitsis RN. Death begets failure in the heart. *J Clin Invest*. 2005;115:565-571
13. Haudek SB, Taffet GE, Schneider MD, Mann DL. Tnf provokes cardiomyocyte apoptosis and cardiac remodeling through activation of multiple cell death pathways. *J Clin Invest*. 2007;117:2692-2701
14. Higami Y, Shimokawa I. Apoptosis in the aging process. *Cell Tissue Res*. 2000;301:125-132
15. van Heerde WL, Robert-Offerman S, Dumont E, Hofstra L, Doevendans PA, Smits JF, Daemen MJ, Reutelingsperger CP. Markers of apoptosis in cardiovascular tissues: Focus on annexin v. *Cardiovasc Res*. 2000;45:549-559
16. Watanabe M, Choudhry A, Berlan M, Singal A, Siwik E, Mohr S, Fisher SA. Developmental remodeling and shortening of the cardiac outflow tract involves myocyte programmed cell death. *Development*. 1998;125:3809-3820
17. Dollery CM, McEwan JR, Henney AM. Matrix metalloproteinases and cardiovascular disease. *Circ Res*. 1995;77:863-868
18. Kim HE, Dalal SS, Young E, Legato MJ, Weisfeldt ML, D'Armiento J. Disruption of the myocardial extracellular matrix leads to cardiac dysfunction. *J Clin Invest*. 2000;106:857-866
19. Spinale FG. Myocardial matrix remodeling and the matrix metalloproteinases: Influence on cardiac form and function. *Physiol Rev*. 2007;87:1285-1342
20. Tyagi SC, Campbell SE, Reddy HK, Tjahja E, Voelker DJ. Matrix metalloproteinase activity expression in infarcted, noninfarcted and dilated cardiomyopathic human hearts. *Mol Cell Biochem*. 1996;155:13-21
21. Nagase H, Woessner JF, Jr. Matrix metalloproteinases. *J Biol Chem*. 1999;274:21491-21494
22. Blankenberg S, Rupprecht HJ, Poirier O, Bickel C, Smieja M, Hafner G, Meyer J, Cambien F, Tiret L, AtheroGene I. Plasma concentrations and genetic variation of matrix metalloproteinase 9 and prognosis of patients with cardiovascular disease. *Circulation*. 2003;107:1579-1585

23. Bonnans C, Chou J, Werb Z. Remodelling the extracellular matrix in development and disease. *Nat Rev Mol Cell Biol*. 2014;15:786-801
24. Chiao YA, Ramirez TA, Zamilpa R, Okoronkwo SM, Dai Q, Zhang J, Jin YF, Lindsey ML. Matrix metalloproteinase-9 deletion attenuates myocardial fibrosis and diastolic dysfunction in ageing mice. *Cardiovasc Res*. 2012;96:444-455
25. Halade GV, Jin YF, Lindsey ML. Matrix metalloproteinase (mmp)-9: A proximal biomarker for cardiac remodeling and a distal biomarker for inflammation. *Pharmacol Ther*. 2013;139:32-40
26. Crean AM, Maredia N, Ballard G, Menezes R, Wharton G, Forster J, Greenwood JP, Thomson JD. 3d echo systematically underestimates right ventricular volumes compared to cardiovascular magnetic resonance in adult congenital heart disease patients with moderate or severe rv dilatation. *J Cardiovasc Magn Reson*. 2011;13:78
27. Ho SY, Nihoyannopoulos P. Anatomy, echocardiography, and normal right ventricular dimensions. *Heart*. 2006;92 Suppl 1:i2-13
28. Orwat S, Diller GP, Baumgartner H. Imaging of congenital heart disease in adults: Choice of modalities. *Eur Heart J Cardiovasc Imaging*. 2014;15:6-17
29. Das NM, Hatsell S, Nannuru K, Huang L, Wen X, Wang L, Wang LH, Idone V, Meganck JA, Murphy A, Economides A, Xie L. In vivo quantitative microcomputed tomographic analysis of vasculature and organs in a normal and diseased mouse model. *PLoS One*. 2016;11:e0150085
30. Jaffer FA, Libby P, Weissleder R. Optical and multimodality molecular imaging: Insights into atherosclerosis. *Arterioscler Thromb Vasc Biol*. 2009;29:1017-1024
31. Kaijzel EL, van Heijningen PM, Wielopolski PA, Vermeij M, Koning GA, van Cappellen WA, Que I, Chan A, Dijkstra J, Ramnath NW, Hawinkels LJ, Bernsen MR, Lowik CW, Essers J. Multimodality imaging reveals a gradual increase in matrix metalloproteinase activity at aneurysmal lesions in live fibulin-4 mice. *Circ Cardiovasc Imaging*. 2010;3:567-577
32. Khamis RY, Woollard KJ, Hyde GD, Boyle JJ, Bicknell C, Chang SH, Malik TH, Hara T, Mauskapf A, Granger DW, Johnson JL, Ntziachristos V, Matthews PM, Jaffer FA, Haskard DO. Near infrared fluorescence (nirf) molecular imaging of oxidized ldl with an autoantibody in experimental atherosclerosis. *Sci Rep*. 2016;6:21785
33. Liang G, Vo D, Nguyen P. Fundamentals of cardiovascular molecular imaging: A review of concepts and strategies. *Curr Cardiovasc Imaging Rep*. 2017;10
34. Agah R, Frenkel PA, French BA, Michael LH, Overbeek PA, Schneider MD. Gene recombination in postmitotic cells. Targeted expression of cre recombinase provokes cardiac-restricted, site-specific rearrangement in adult ventricular muscle in vivo. *J Clin Invest*. 1997;100:169-179
35. Kirschner K, Singh R, Prost S, Melton DW. Characterisation of ercc1 deficiency in the liver and in conditional ercc1-deficient primary hepatocytes in vitro. *DNA Repair (Amst)*. 2007;6:304-316
36. Moore RC, Redhead NJ, Selfridge J, Hope J, Manson JC, Melton DW. Double replacement gene targeting for the production of a series of mouse strains with different prion protein gene alterations. *Biotechnology (N Y)*. 1995;13:999-1004
37. Vermeij WP, Dolle ME, Reiling E, Jaarsma D, Payan-Gomez C, Bombardieri CR, Wu H, Roks AJ, Botter SM, van der Eerden BC, Youssef SA, Kuiper RV, Nagarajah B, van Oostrom CT, Brandt RM, Barnhoorn S, Imholz S, Pennings JL, de Bruin A, Gyenis A, Pothof J, Vijg J, van Steeg H, Hoeijmakers JH. Restricted diet delays accelerated ageing and genomic stress in DNA-repair-deficient mice. *Nature*. 2016;537:427-431
38. Houser SR, Margulies KB, Murphy AM, Spinale FG, Francis GS, Prabhu SD, Rockman HA, Kass DA, Molkentin JD, Sussman MA, Koch WJ, American Heart Association Council on Basic

Cardiovascular Sciences CoCC, Council on Functional G, Translational B. Animal models of heart failure: A scientific statement from the american heart association. *Circ Res*. 2012;111:131-150

39. Mirzaei H, Di Biase S, Longo VD. Dietary interventions, cardiovascular aging, and disease: Animal models and human studies. *Circ Res*. 2016;118:1612-1625
40. Coughlin SS, Tefft MC, Rice JC, Gerone JL, Baughman KL. Epidemiology of idiopathic dilated cardiomyopathy in the elderly: Pooled results from two case-control studies. *Am J Epidemiol*. 1996;143:881-888
41. Kono Y, Nakamura K, Kimura H, Nishii N, Watanabe A, Banba K, Miura A, Nagase S, Sakuragi S, Kusano KF, Matsubara H, Ohe T. Elevated levels of oxidative DNA damage in serum and myocardium of patients with heart failure. *Circ J*. 2006;70:1001-1005
42. Li YY, Hengstenberg C, Maisch B. Whole mitochondrial genome amplification reveals basal level multiple deletions in mtdna of patients with dilated cardiomyopathy. *Biochem Biophys Res Commun*. 1995;210:211-218
43. Wang J, Wilhelmsson H, Graff C, Li H, Oldfors A, Rustin P, Bruning JC, Kahn CR, Clayton DA, Barsh GS, Thoren P, Larsson NG. Dilated cardiomyopathy and atrioventricular conduction blocks induced by heart-specific inactivation of mitochondrial DNA gene expression. *Nat Genet*. 1999;21:133-137
44. Zhang D, Mott JL, Farrar P, Ryerse JS, Chang SW, Stevens M, Denniger G, Zassenhaus HP. Mitochondrial DNA mutations activate the mitochondrial apoptotic pathway and cause dilated cardiomyopathy. *Cardiovasc Res*. 2003;57:147-157
45. Dai DF, Rabinovitch PS, Ungvari Z. Mitochondria and cardiovascular aging. *Circ Res*. 2012;110:1109-1124
46. Ishida T, Ishida M, Tashiro S, Yoshizumi M, Kihara Y. Role of DNA damage in cardiovascular disease. *Circ J*. 2014;78:42-50
47. Mondal NK, Sorensen E, Hiivala N, Feller E, Griffith B, Wu ZJ. Oxidative stress, DNA damage and repair in heart failure patients after implantation of continuous flow left ventricular assist devices. *Int J Med Sci*. 2013;10:883-893
48. Shukla PC, Singh KK, Yanagawa B, Teoh H, Verma S. DNA damage repair and cardiovascular diseases. *Can J Cardiol*. 2010;26 Suppl A:13A-16A
49. Tsutsui H, Ide T, Kinugawa S. Mitochondrial oxidative stress, DNA damage, and heart failure. *Antioxid Redox Signal*. 2006;8:1737-1744
50. Dolle ME, Kuiper RV, Roodbergen M, Robinson J, de Vlugt S, Wijnhoven SW, Beems RB, de la Fonteyne L, de With P, van der Pluijm I, Niedernhofer LJ, Hasty P, Vijg J, Hoeijmakers JH, van Steeg H. Broad segmental progeroid changes in short-lived ercc1(-/delta7) mice. *Pathobiol Aging Age Relat Dis*. 2011;1
51. Gregg SQ, Robinson AR, Niedernhofer LJ. Physiological consequences of defects in ercc1-xpf DNA repair endonuclease. *DNA Repair (Amst)*. 2011;10:781-791
52. de Waard MC, van der Pluijm I, Zuiderveen Borgesius N, Comley LH, Haasdijk ED, Rijksen Y, Ridwan Y, Zondag G, Hoeijmakers JH, Elgersma Y, Gillingwater TH, Jaarsma D. Age-related motor neuron degeneration in DNA repair-deficient ercc1 mice. *Acta Neuropathol*. 2010;120:461-475
53. Spoor M, Nagtegaal AP, Ridwan Y, Borgesius NZ, van Alphen B, van der Pluijm I, Hoeijmakers JH, Frens MA, Borst JG. Accelerated loss of hearing and vision in the DNA-repair deficient ercc1(delta/-) mouse. *Mech Ageing Dev*. 2012;133:59-67

54. Gurkar AU, Niedernhofer LJ. Comparison of mice with accelerated aging caused by distinct mechanisms. *Exp Gerontol*. 2015;68:43-50
55. Tsui BM, Kraitchman DL. Recent advances in small-animal cardiovascular imaging. *J Nucl Med*. 2009;50:667-670
56. Badea CT, Fubara B, Hedlund LW, Johnson GA. 4-d micro-ct of the mouse heart. *Mol Imaging*. 2005;4:110-116
57. Drangova M, Ford NL, Detombe SA, Wheatley AR, Holdsworth DW. Fast retrospectively gated quantitative four-dimensional (4d) cardiac micro computed tomography imaging of free-breathing mice. *Invest Radiol*. 2007;42:85-94
58. Ma Y, Chiao YA, Clark R, Flynn ER, Yabluchanskiy A, Ghasemi O, Zouein F, Lindsey ML, Jin YF. Deriving a cardiac ageing signature to reveal mmp-9-dependent inflammatory signalling in senescence. *Cardiovasc Res*. 2015;106:421-431
59. Yabluchanskiy A, Ma Y, Chiao YA, Lopez EF, Voorhees AP, Toba H, Hall ME, Han HC, Lindsey ML, Jin YF. Cardiac aging is initiated by matrix metalloproteinase-9-mediated endothelial dysfunction. *Am J Physiol Heart Circ Physiol*. 2014;306:H1398-1407
60. Bonnema DD, Webb CS, Pennington WR, Stroud RE, Leonardi AE, Clark LL, McClure CD, Finklea L, Spinale FG, Zile MR. Effects of age on plasma matrix metalloproteinases (mmps) and tissue inhibitor of metalloproteinases (timps). *J Card Fail*. 2007;13:530-540
61. Chiao YA, Dai Q, Zhang J, Lin J, Lopez EF, Ahuja SS, Chou YM, Lindsey ML, Jin YF. Multi-analyte profiling reveals matrix metalloproteinase-9 and monocyte chemotactic protein-1 as plasma biomarkers of cardiac aging. *Circ Cardiovasc Genet*. 2011;4:455-462
62. Campisi J. Aging, cellular senescence, and cancer. *Annu Rev Physiol*. 2013;75:685-705
63. Childs BG, Durik M, Baker DJ, van Deursen JM. Cellular senescence in aging and age-related disease: From mechanisms to therapy. *Nat Med*. 2015;21:1424-1435
64. Koda M, Takemura G, Kanoh M, Hayakawa K, Kawase Y, Maruyama R, Li Y, Minatoguchi S, Fujiwara T, Fujiwara H. Myocytes positive for in situ markers for DNA breaks in human hearts which are hypertrophic, but neither failed nor dilated: A manifestation of cardiac hypertrophy rather than failure. *J Pathol*. 2003;199:229-236
65. Olivetti G, Abbi R, Quaini F, Kajstura J, Cheng W, Nitahara JA, Quaini E, Di Loreto C, Beltrami CA, Krajewski S, Reed JC, Anversa P. Apoptosis in the failing human heart. *N Engl J Med*. 1997;336:1131-1141
66. Saraste A, Pulkki K, Kallajoki M, Heikkila P, Laine P, Mattila S, Nieminen MS, Parvinen M, Voipio-Pulkki LM. Cardiomyocyte apoptosis and progression of heart failure to transplantation. *Eur J Clin Invest*. 1999;29:380-386
67. Takemura G, Kanoh M, Minatoguchi S, Fujiwara H. Cardiomyocyte apoptosis in the failing heart--a critical review from definition and classification of cell death. *Int J Cardiol*. 2013;167:2373-2386
68. Kanoh M, Takemura G, Misao J, Hayakawa Y, Aoyama T, Nishigaki K, Noda T, Fujiwara T, Fukuda K, Minatoguchi S, Fujiwara H. Significance of myocytes with positive DNA in situ nick end-labeling (tunel) in hearts with dilated cardiomyopathy: Not apoptosis but DNA repair. *Circulation*. 1999;99:2757-2764